ESO Science Archive Facility - Phase 3 Data Release Description
ESO public survey programme VPHAS+ - VST Photometric H-a Survey of the Southern Galactic Plane, Data Release DR3.1
provided by Janet Drew, submitted between 2017-05-30 and 2017-08-14, published on 2017-08-17

ESO Phase 3 Data Release Description

Data Collection	VPHASplus
Release Number	3.1
Data Provider	J. E. Drew, N. Cross, M. Read, R. Raddi
Date	14.08.2017

Abstract

This document describes the released VPHAS+ DR3 Source Catalogue (VPHAS-DR3-PSC), which is a superseding band- and field-merged science catalogue created from the imaging data obtained by the VST Photometric H-alpha Survey of the Southern Galactic Plane and Bulge (VPHAS+).

The primary goal of VPHAS+ is to collect single-epoch ugri broad-band and H-alpha narrow-band photometry across the southern Galactic Plane within the latitude range $-5^{o} < b < +5^{o}$ down to source magnitudes of ~21. The VPHAS+ footprint also includes the inner Galactic Bulge, defined as a 20 x 20 sq.deg box around the Galactic Centre: this assures optical coverage of the full VVV footprint. For all massive OBA stars this survey is deep enough to explore all but the most heavily obscured locations of the southern Plane, reaching to 4—10 kpc from the Sun. VPHAS+ will increase the number of known southern emission line stars of all types by up to an order of magnitude, yielding much better statistics on important short-lived object classes. The wide-area uniform photometry obtained will also facilitate stellar population studies, capable of tracing structure over much of the southern Plane. VPHAS+ is designed for trawling the star-formation history of the Galaxy as seen in white dwarfs and other stellar remnants.

A leading survey goal is the production of a well-validated catalogue that provides 5 optical photometric data points per Galactic Plane source at an external (systematic) precision of 0.02—0.03 magnitudes. This released data product is the next step on the way to such a catalogue, providing aperture photometry for 529 million primary detections, against a rough global calibration in the g, r and i bands, using APASS as a reference survey. The number of unique objects is lower than this total (~300 million), since the method of catalogue preparation does not completely remove all duplicates gathered in >2 exposures/filter/position over most of the southern Plane.

The catalogue presented here is derived from the reduced photometry and images that have been released as the "VPHAS-DR2" collection and all but the last 6 months of "VPHAS-DR3". It covers data-taking up to 30/03/2015, by which time 39% of all survey filter-sets had been observed to sufficient quality. Magnitudes are expressed in the AB scale. These observations were taken under ESO programme 177.D-3023(B,C,D,E,F,G,H).

This release also includes a pair of images and source lists missed from the imaging DR3 (red-filter r exposures for field 1251, centred on Galactic coordinates 338.41, +1.44).

Overview of Observations

Since the observations are a subset of those included in the "VPHAS-DR2" and "VPHAS-DR3" releases of imaging data, the reader is referred to the VPHAS-DR3 release description for information on data taking and data quality statistics. The URLs are

http://www/eso.org/rm/api/v1/public/releaseDescriptions/53

and

http://www.eso.org/rm/api/v1/public/releaseDescriptions/86

A map of the included pointings in this release is shown as figure 1.

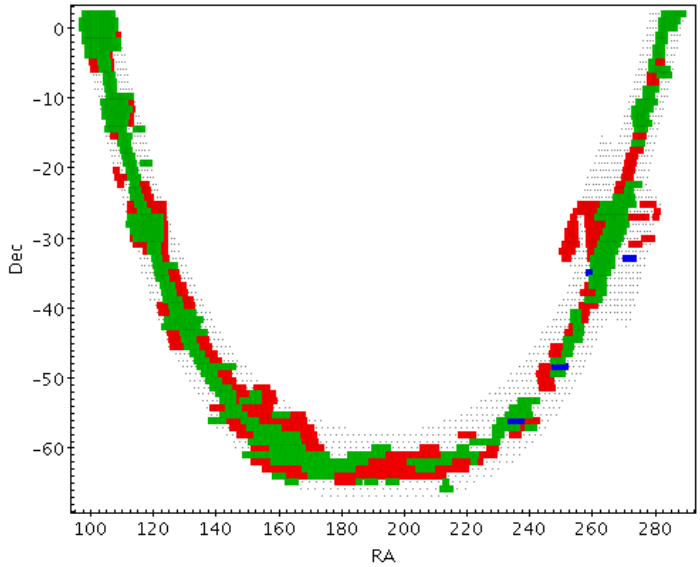

Figure 1: Map of the DR3-released pointings. Fields observed in all filters are shown in green. Red colours are used where only Ha/r/i data are included, and blue for u/g/r only. The grey dots indicate the rest of the survey footprint.

Release Content

This release provides a band-merged catalogue covering roughly 1100 deg^2 (48%) of the VPHAS+ footprint, i.e. the Southern Galactic plane. As shown above in figure 1, the Galactic mid-plane is very nearly complete. All data obtained by March 30th, 2015, are included.

The catalogue is built from 3.052 billion measurements across all 5 filters. The number of catalogue rows is 904.2 million, with each row detailing the detection of an object in one or both of two contemporaneous filter sets: a u/g/r exposure set, and an r/i/Ha set. For practical scheduling reasons, the sequence of u/g/r ("blue") exposures are, with very few exceptions, acquired on a different night from the sequence of r/i/Ha ("red") exposures. Nevertheless, the blue and red filter sets within themselves are gathered within concatenations completed within 40-50 mins, in order that faithful u-g,g-r and r-Ha,r-i photometric diagrams can be guaranteed.

Because the r band is included in both the blue and the red filter sequences, there are two exposures available in this filter at each telescope pointing. In the catalogue we define "r" as the r-band magnitude obtained with the Ha and i filter exposures, and "r2" as the r-band magnitude collected with u and g. More rows in the catalogue contain both r and r2 magnitudes than do not. But, in this release, the overall sky area observed in the red filters continues to be significantly *in advance of* that ob*served in blue filters*: as a result, almost 40% of rows in the catalogue show values for r/i/Ha only, while for a few *only*, *just* u/g/r2 data are provided. A point of detail: this release also includes a pair of images and source lists that were missed from the imaging DR3 (red-filter r exposures for field 1251, centred on Galactic coordinates 338.41, +1.44).

Catalogue columns are set aside for contemporaneous colours: these are derived from within the appropriate filter set (u-g, g-r2, from u/g/r2 concatenations; r-Ha, r-i from r/i/Ha).

The survey observing pattern comprises offset pointings of up to 11 arcmin in order to compensate for inter-CCD gaps and to better sample the known variation of the segmented NB-659 transmission profile across the image plane (the details of this were discussed in Drew et al 2014). As a result, the great majority of stars in the footprint are each captured by 2 or 3 different telescope pointings in each band, with the resultant detections feeding into multiple rows in the

catalogue. Advice is provided later in this document to aid the user in identifying the best available detection set per unique object.

In this release, the third exposures taken at an intermediate offset in the g and Ha bands are, per field, combined into a third frameset (alongside the two u/g/r2/r/i/Ha framesets constructed otherwise as standard). These three framesets per field constitute a tile.

The catalogue's magnitude limits vary across the footprint, being influenced especially by source crowding, as well as by seeing. The typical 5-sigma limits range from around 20.7 in the Ha narrowband up to 22.5 in g. There is a strong gradient in the number of detections per filter, such that e.g. the u band count is around an order of magnitude smaller than the count in i band. Table 1 below reports the exact number of catalogue measurements by pass band and offers round-number estimates for the number of unique sources they represent.

Pass band	# measurements (millions)	# unique sources (millions)
u	83.3	40
g	310.1	100
r and r2	999.3	200
Ha (NB_659)	845.7	220
i	813.6	330

Table1: Data on numbers of detections in the DR3 catalogue by pass band.

The final column yields the expected pattern – given both rising interstellar extinction with decreasing wavelength and the intrinsically red colour of the numerically dominant cool stars.

Release Notes

Data Reduction and Calibration

Please see the description of the data reduction provided in the release document accompanying the DR3 collection of single-band flux lists and reduced images. See also the original survey paper (Drew et al 2014, MNRAS, 440, 2036).

A preliminary global calibration of the aperture photometry in the g/r/i bands has been obtained as a by-product of the CASU pipeline illumination correction step. In these bands, the pipeline makes a direct comparison with APASS, thereby mapping the VPHAS+ photometric scale onto the APASS AB system. This is carried through to the catalogue: to place into the alternative Vega system, the representative shifts given in table 2 below should be **added** to the catalogue magnitudes.

Photometric band	Typical AB→Vega shift
U	-0.79
G	+0.10
r, r2	-0.15
Ha (NB_659)	-0.27
I	-0.38

Table 2: Representative values for the corrections from DR3 catalogue AB magnitudes to the Vega zero magnitude scale.

Tests on large selections (many sq.deg each) from the catalogue indicate that the like-for-like DR3 and already-released DR2 aperture photometry are approximately aligned, and will deliver broadly compatible colour-colour diagrams. However the calibration at present is preliminary, and remains subject to field-to-field shifts on scales of up to 0.05 magnitudes often, and occasionally more (see next sections and figure 2). This is especially true of the Ha and u bands that presently rely on inter- or extrapolation from the APASS-referenced g/r/i bands. The data in all

bands still await iteration to a uniform system through reconciliation of field overlaps: this will be undertaken as the survey observations approach completion. At the present time, source selections over angular ranges exceeding the 1 sq.deg VST OmegaCAM footprint will usually exhibit more scatter than localized selections exploiting a common calibration.

Data Quality

This is the second band-merged science catalogue to have been created for the VPHAS+ survey, and the first to pass through the data flow managed by WFAU Edinburgh. In many respects, the method of catalogue generation is the same as applied to the VST ATLAS survey, which in turn re-uses the VISTA Data Flow System (Hambly et al 2008 MNRAS 384 637; Cross et al 2012 A&A 548 A119).

Referring the DR3 g/r/i photometric scale to the APASS survey does not yet assure a stable uniform scale: absolute scale field-to-field drifts of 0.03—0.05 mag in these bands are certainly present and may on very rare occasions reach 0.1-0.5 mag. These drifts are most troublesome in the crowded fields around the Galactic Centre where it is more likely that source confusion in APASS compromises the calibration step. Figure 2 below provides the results of an inter-comparison between DR3 and IPHAS DR2 (panels a and c, Barentsen et al 2014 MNRAS 444 3230) and also DR3 and VPHAS+ DR2 (panels b and d). The selections shown are located on the celestial equator at opposite ends of the VPHAS+ footprint (see figure 1).

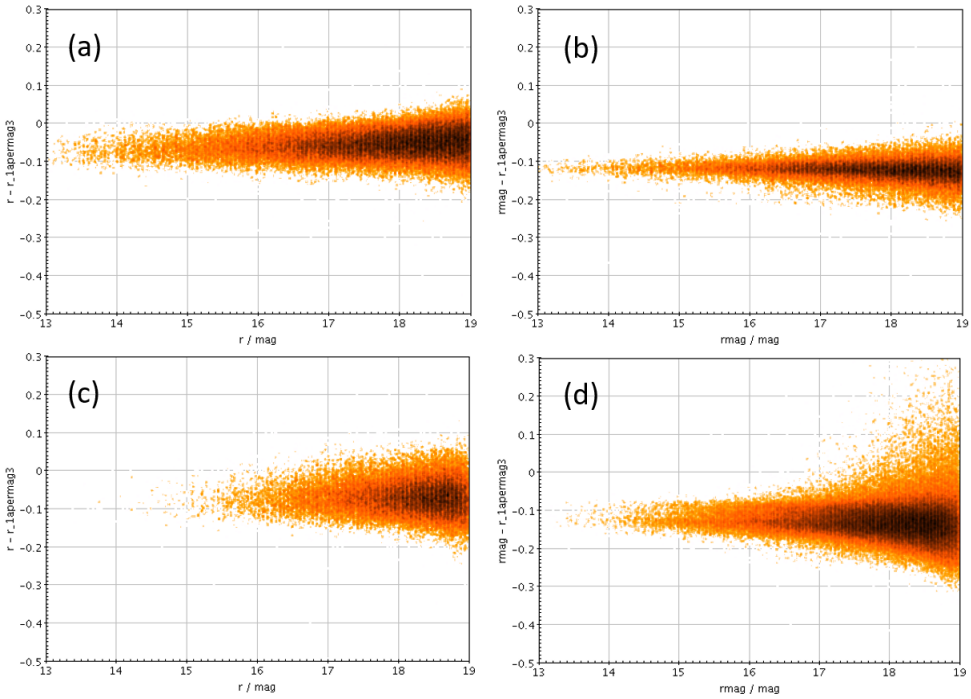

Figure 2: In the top row, r band magnitudes in the DR3 catalogue obtained from a 1-degree radius cone selection centered on l = 213°, b = 0.0° are compared directly with (a) IPHAS DR2 r (A10POINT=1), (b) VPHAS+ DR2 r (CLEAN=1). These are point-density plots such that the dark brown colour is associated with the highest point density, fading to white at lowest density. In all cases, the variable on the vertical axis is the difference between the AB DR3 magnitude and the Vega magnitude derived from IPHAS or VPHAS+ DR2 (as supplied by Vizier): the expected mean of this difference is –0.15 mags. Notice that the VPHAS+ DR2 and DR3 selections compared in panel (b) are based on the same VST observations – they differ in cross-matching strategy and method of photometric calibration. In these examples, the AB to Vega mean shifts illustrated differ by ~0.05 mags and neither is as negative as the recommended –0.15. Panels (c) and (d) are analogous plots for a 1-degree radius cone selection at l = 33°, b=0.0° at the opposite end of the VPHAS+ footprint, where source densities are typically several times higher and the influence of Southern-winter observing conditions is apparent. Again the mean AB-Vega offsets are different in (c) and (d), and there is evi-

dence in panel (d) of a calibration offset within the selected data – there is also greater scatter at fainter magnitudes relative to panel (b).

Known issues

1) OmegaCAM CCD extension number 10 (formal name "ESO_CCD_82") is known to have suffered from significant gain variations from the start of VST operations up until 2 June 2012.
2) There are gaps between the 32 CCDs making up the OmegaCAM mosaic that impose a pattern of dead strips on the obtained images. The offsetting strategy reduces these to a bare minimum, but very small completely unexposed patches remain within the survey footprint. These are greatest in Ha data, thanks to the greater vignetting of the segmented filter, but still only amount to around 0.3 percent. Furthermore the overall pattern of sky coverage (figure 1) remains irregular. It is recommended to always inspect plots of the sky distribution of selected sources before beginning exploitation, so that area incompleteness is understood from the outset of use.
3) The pointing of the VST occasionally deviates from request enough to cause blue+red sequences to be misaligned by up to ~10%. This complicates the pattern of field overlap but should not lead to much source loss.
4) The third g and Ha pointings obtained at an intermediate offset between the offsets used for u,r and i appear in the present catalogue as additional detections and are not merged into the framesets from which the primary bandmerged detections are selected – the latter includes up to 6 detections from u to i.

Advice to users of the catalogue

See the Appendix for specifications of all catalogue columns.

Catalogue users, interested in sky areas well below the OmegaCAM1 sq.deg. field, are advised to use the observation date columns to select source detections obtained within the same concatenation: such data will all be on exactly the same photometric scale. In particular, colours involving the u and Ha bands should then exhibit an internal consistency that may otherwise be somewhat degraded. As an example, it would not be surprising to find (r-i, r-Ha) diagrams exhibit sequences split in r-Ha when the data plotted combine observations from different fields/nights. When effects of this kind are noticed, the user is advised to check his or her method of selection – mindful of the point that split sequences can also arise for good astrophysical reasons (e.g. the existence of a pronounced intervening layer of interstellar dust along the line of sight).

Setting the constraint, PRIMARY = 1, picks out data with the following properties from among available duplicates:

- ppErrBits not greater than 256 in any band – first applied criterion
- largest number of filter measurements (e.g. the existence of u/g/r2/r/Ha/i detections would be favoured over the shorter list, g/r2/r/Ha/i).
- the detection closest to the OmegaCam optical axis – last applied criterion

This selection does not guarantee a list of *unique* objects. An option for investigating this further would be to crossmatch a PRIMARY = 1 selection with itself, demanding maximum separations not more than ~0.2 arcsec, in order to enumerate close pairs that may be duplicates derived from different fields or exposures.

Users are also reminded that 3rd g and Ha intermediate-offset exposures are presently compiled into separate framesets and will not be designated as PRIMARY, in the presence of the compilations of u/g/r2/r/i/Ha measurements at nearly-identical coordinates. Again, cross-matching can find these out.

DR3 catalogue data are also available at the OmegaCAM Science Archive (http://osa.roe.ac.uk , problems/queries email point of contact: osa-support@roe.ac.uk).

Previous Releases

The DR2 catalogue preceding this one is now available via the CDS Vizier pages (see http://cdsarc.u-strasbg.fr/viz-bin/Cat?II/341). This release supersedes in that it includes the sky area covered in DR2, but it is important to note that it provides aperture photometry only – as produced by the CASU data pipeline. The DR2 catalogue included tailored list-driven PSF photometry that, in crowded areas especially, will be more reliable than the magnitude data provided in DR3. Hence, continued use of the older catalogue is recommended for the highest stellar density applications.

Data Format

File Types

This bandmerged catalogue was prepared by the Wide Field Astronomy Unit (WFAU), Edinburgh. It contains a subset of the parameters as supplied in the CASU lists, but with magnitudes in place of fluxes and with contemporaneous colours added. Additional parameters include some useful statistics providing information on the nature of each source detection (e.g. date of observation, a merged classification code, measures of single-band point-spread-function properties). The data files are based on framesets formed by merging catalogues from individual detectors. The catalogue is made up from 1092 tiles, each one covering 1.32 sq.deg. The total required storage is ~0.44 terabytes.

Acknowledgements

The general journal reference for VPHAS+ is: Drew et al, 2014, MNRAS, 440, 2036.

If making use of data from this catalogue in a publication, please use the following statement in the acknowledgements: "The VPHAS DR3 catalogue is based on data products from observations made with ESO Telescopes at the La Silla Paranal Observatory under public survey programme ID, 177.D-3023" .

Appendix: Catalogue Column Names and Descriptors

Column; Name; FITS data type; Description

1:IAUNAME; 31A; IAU Name (not unique)
2:sourceID; K; UID (unique over entire OSA via programme ID prefix) of this merged detection as assigned by merge algorithm
3:ra2000; D; Celestial Right Ascension
4:dec2000; D; Celestial Declination
5:l; D; Galactic longitude
6:b; D; Galactic latitude
7:mergedClass; I; Class flag from available measurements (1|0|-1|-2|-3|-9=galaxy|noise|stellar|probableStar|probableGalaxy|saturated)
8:umgPnt; E; Point source colour u-g (using aperMag3)
9:umgPntErr; E; Error on point source colour u-g
10:gmr2Pnt; E; Point source contemporary colour g-r2 (using aperMag3) from ugr epoch
11:gmr2PntErr; E; Error on point source colour g-r2
12:rmhavphasPnt;E; Point source contemporary colour r-Halpha (using aperMag3) from riHa epoch
13:rmhavphasPntErr;E; Error on point source colour r-Halpha

14:rmiPnt; E; Point source contemporary colour r-i (using aperMag3) from riHa epoch
15:rmiPntErr; E; Error on point source colour r-i
16:uMjd; D; The mean Modified Julian Day of each detection
17:uAperMag3; E; Default point source u aperture corrected mag (2.0 arcsec aperture diameter)
18:uAperMag3Err; E; Error in default point/extended source u mag (2.0 arcsec aperture diameter)
19:uAperMag4; E; Point source u aperture corrected mag (2.8 arcsec aperture diameter)
20:uAperMag4Err; E; Error in point/extended source u mag (2.8 arcsec aperture diameter)
21:uAperMag6; E; Point source u aperture corrected mag (5.7 arcsec aperture diameter)
22:uAperMag6Err; E; Error in point/extended source u mag (5.7 arcsec aperture diameter)
23:uGausig; E; RMS of axes of ellipse fit in u
24:uEll; E; 1-b/a, where a/b=semi-major/minor axes in u
25:uPA; E; ellipse fit celestial orientation in u
26:uErrBits; J; processing warning/error bitwise flags in u
27:uppErrBits; J; additional WFAU post-processing error bits in u
28:uAverageConf; E; average confidence in 2 arcsec diameter default aperture (aper3) u
29:uClass; I; discrete image classification flag in u
30:uXi; E; Offset of u detection from master position (+east/-west)
31:uEta; E; Offset of u detection from master position (+north/-south)
32:uSeqNum; J; the running number of the u detection
33:gMjd; D; The mean Modified Julian Day of each detection
34:gAperMag3; E; Default point source g aperture corrected mag (2.0 arcsec aperture diameter)
35:gAperMag3Err; E; Error in default point/extended source g mag (2.0 arcsec aperture diameter)
36:gAperMag4; E; Point source g aperture corrected mag (2.8 arcsec aperture diameter)
37:gAperMag4Err; E; Error in point/extended source g mag (2.8 arcsec aperture diameter)
38:gAperMag6; E; Point source g aperture corrected mag (5.7 arcsec aperture diameter)
39:gAperMag6Err; E; Error in point/extended source g mag (5.7 arcsec aperture diameter)
40:gGausig; E; RMS of axes of ellipse fit in g
41:gEll; E; 1-b/a, where a/b=semi-major/minor axes in g
42:gPA; E; ellipse fit celestial orientation in g
43:gErrBits; J; processing warning/error bitwise flags in g
44:gppErrBits; J; additional WFAU post-processing error bits in g
45:gAverageConf; E; average confidence in 2 arcsec diameter default aperture (aper3) g
46:gClass; I; discrete image classification flag in g
47:gXi; E; Offset of g detection from master position (+east/-west)
48:gEta; E; Offset of g detection from master position (+north/-south)
49:gSeqNum; J; the running number of the g detection
50:r2Mjd; D; The mean Modified Julian Day of each detection
51:r2AperMag3; E; Default point source r2 aperture corrected mag (2.0 arcsec aperture diameter)
52:r2AperMag3Err; E; Error in default point/extended source r2 mag (2.0 arcsec aperture diameter)
53:r2AperMag4; E; Point source r2 aperture corrected mag (2.8 arcsec aperture diameter)
54:r2AperMag4Err; E; Error in point/extended source r2 mag (2.8 arcsec aperture diameter)
55:r2AperMag6; E; Point source r2 aperture corrected mag (5.7 arcsec aperture diameter)
56:r2AperMag6Err; E; Error in point/extended source r2 mag (5.7 arcsec aperture diameter)
57:r2Gausig; E; RMS of axes of ellipse fit in r2
58:r2Ell; E; 1-b/a, where a/b=semi-major/minor axes in r2
59:r2PA; E; ellipse fit celestial orientation in r2
60:r2ErrBits; J; processing warning/error bitwise flags in r2
61:r2ppErrBits; J; additional WFAU post-processing error bits in r2
62:r2AverageConf; E; average confidence in 2 arcsec diameter default aperture (aper3) r2
63:r2Class; I; discrete image classification flag in r2
64:r2Xi; E; Offset of r2 detection from master position (+east/-west)
65:r2Eta; E; Offset of r2 detection from master position (+north/-south)
66:r2SeqNum; J; the running number of the r2 detection
67:rMjd; D; The mean Modified Julian Day of each detection
68:rAperMag3; E; Default point source r aperture corrected mag (2.0 arcsec aperture diameter)

69:rAperMag3Err; E; Error in default point/extended source r mag (2.0 arcsec aperture diameter)
70:rAperMag4; E; Point source r aperture corrected mag (2.8 arcsec aperture diameter)
71:rAperMag4Err; E; Error in point/extended source r mag (2.8 arcsec aperture diameter)
72:rAperMag6; E; Point source r aperture corrected mag (5.7 arcsec aperture diameter)
73:rAperMag6Err; E; Error in point/extended source r mag (5.7 arcsec aperture diameter)
74:rGausig; E; RMS of axes of ellipse fit in r
75:rEll; E; 1-b/a, where a/b=semi-major/minor axes in r
76:rPA; E; ellipse fit celestial orientation in r
77:rErrBits; J; processing warning/error bitwise flags in r
78:rppErrBits; J; additional WFAU post-processing error bits in r
79:rAverageConf; E; average confidence in 2 arcsec diameter default aperture (aper3) r
80:rClass; I; discrete image classification flag in r
81:rXi; E; Offset of r detection from master position (+east/-west)
82:rEta; E; Offset of r detection from master position (+north/-south)
83:rSeqNum; J; the running number of the r detection
84:iMjd; D; The mean Modified Julian Day of each detection
85:iAperMag3; E; Default point source i aperture corrected mag (2.0 arcsec aperture diameter)
86:iAperMag3Err; E; Error in default point/extended source i mag (2.0 arcsec aperture diameter)
87:iAperMag4; E; Point source i aperture corrected mag (2.8 arcsec aperture diameter)
88:iAperMag4Err; E; Error in point/extended source i mag (2.8 arcsec aperture diameter)
89:iAperMag6; E; Point source i aperture corrected mag (5.7 arcsec aperture diameter)
90:iAperMag6Err; E; Error in point/extended source i mag (5.7 arcsec aperture diameter)
91:iGausig; E; RMS of axes of ellipse fit in i
92:iEll; E; 1-b/a, where a/b=semi-major/minor axes in i
93:iPA; E; ellipse fit celestial orientation in i
94:iErrBits; J; processing warning/error bitwise flags in i
95:ippErrBits; J; additional WFAU post-processing error bits in i
96:iAverageConf; E; average confidence in 2 arcsec diameter default aperture (aper3) i
97:iClass; I; discrete image classification flag in i
98:iXi; E; Offset of i detection from master position (+east/-west)
99:iEta; E; Offset of i detection from master position (+north/-south)
100:iSeqNum; J; the running number of the i detection
101:havphasMjd; D; The mean Modified Julian Day of each detection
102:havphasAperMag3; E; Default point source Havphas aperture corrected mag (2.0 arcsec aperture diameter)
103:havphasAperMag3Err; E; Error in default point source Havphas mag (2.0 arcsec aperture diameter)
104:havphasAperMag4; E; Point source Havphas aperture corrected mag (2.8 arcsec aperture diameter)
105:havphasAperMag4Err; E; Error in point source Havphas mag (2.8 arcsec aperture diameter)
106:havphasAperMag6; E; Point source Havphas aperture corrected mag (5.7 arcsec aperture diameter)
107:havphasAperMag6Err; E; Error in point source Havphas mag (5.7 arcsec aperture diameter)
108:havphasGausig; E; RMS of axes of ellipse fit in Havphas
109:havphasEll; E; 1-b/a, where a/b=semi-major/minor axes in Havphas
110:havphasPA; E; ellipse fit celestial orientation in Havphas
111:havphasErrBits; J; processing warning/error bitwise flags in Havphas
112:havphasppErrBits; J; additional WFAU post-processing error bits in Havphas
113:havphasAverageConf; E; average confidence in 2 arcsec diameter default aperture (aper3) Havphas
114:havphasClass; I; discrete image classification flag in Havphas
115:havphasXi; E; Offset of Havphas detection from master position (+east/-west)
116:havphasEta; E; Offset of Havphas detection from master position (+north/-south)
117:havphasSeqNum; J; the running number of the Havphas detection
118:PRIMARY_SOURCE; B; Primary source 1; secondary source 0